An Algorithm for Harsh Doppler Shift Estimation for Satellite Communications

Citation for the original published paper (version of record):
Bezerra de Freitas Diniz, A., Eriksson, T., Gustavsson, U. (2024). An Algorithm for Harsh Doppler Shift Estimation for Satellite Communications. Conference Record - Asilomar Conference on Signals, Systems and Computers: 706-710.
http://dx.doi.org/10.1109/IEEECONF60004.2024.10943109

An Algorithm for Harsh Doppler Shift Estimation for Satellite Communications

André B. de F. Diniz*†, Thomas Eriksson*, and Ulf Gustavsson*†
*Department of Electrical Engineering, Chalmers University of Technology, Gothenburg, Sweden
†Ericsson Research, Gothenburg, Sweden
Email: *{andredin, thomase}@chalmers.se, †ulf.gustavsson@ericsson.com

***Abstract*—Future communication generations are expected to employ low Earth orbit satellites as a complement to current terrestrial networks. Due to the relatively high speeds of these satellites, harsh Doppler shifts are expected to occur during transmission to a base station on Earth. For use with, e.g., internet of things, lower sampling frequencies at the receiver side might be applied, making the normalized Doppler shifts more severe. In this work, we consider a mathematical formulation of the observed Doppler shift by a ground station as a function of the orbital parameters of the satellite. Based on this description, we propose a standalone model- and pilot-based procedure to estimate normalized Doppler shifts that become larger as the sampling frequency decreases, comprising a simple coarse estimation followed by a refinement stage, which applies linear estimators with consecutively longer data blocks. Simulations show practically unbiased estimates of the strongest observed Doppler shift during a satellite pass, reaching the Cramér-Rao lower bound for a wide range of signal-to-noise ratios.**

***Index Terms*—Doppler shift, Satellite communications, model-based processing.**

I. Introduction

In current communication systems, terrestrial networks (TNs) play a vital role in serving more than 4 billion users worldwide [1]. These structures, in 6G and beyond generations, will not be sufficient to provide service with progressively higher demands and number of users, especially in under-covered areas. In this context, non-terrestrial networks appear as a solution to complement the TNs, contributing to, e.g., global coverage, high bandwidth and low latency [2]. To achieve such requirements, the deployment of low Earth orbit (LEO) satellites is expected to be of great importance due to, for instance, their capability of serving densely populated areas and lower delay with respect to satellites at higher altitudes [3].

The high speed of LEO satellites, however, gives rise to a strong Doppler effect, which may generate inter-carrier interference in systems based on orthogonal frequency division multiplexing (OFDM), for instance [4]. The normalized Doppler shifts vary significantly with the satellite position and the system bandwidth. In addition, they become increasingly more severe with lower sampling frequencies at the receiver side. This can be the case, for example, in systems for applications in internet of things. Estimating Doppler shifts using relatively simple methods, even in such harsh conditions, is, thus, of considerable relevance for future networks.

The characterization of Doppler shifts for LEO satellites in circular orbits transmitting towards a base station on Earth, as a function of local geometric variables, has been thoroughly studied in [5], [6]. Furthermore, the Doppler shift as a function of the satellite orbital parameters has been discussed in [7], [8]. Although these models provide a closed-form representation of the Doppler shift during a satellite pass, at least knowledge of the local geometry or the orbital parameters is necessary for compensation of the Doppler effect.

In [9], the structure of the primary synchronization signal (PSS) of 5G frames is explored to provide estimates of Doppler shifts and Doppler rates. For the former, the phase of the received and PSS signals is explored to estimate the fractional Doppler, followed by the peak of the cross-correlation of the compensated PSS and the received signal to estimate the integer part. Especially in noisy scenarios, estimating frequencies using the phase of received signals can be problematic due to unwrapping problems [10]. In addition, currently there is no standard for synchronization structures for future 6G systems, so algorithms that take advantage of PSS within OFDM frames may not be utilized in the upcoming generations.

We propose a simple method for estimation of Doppler shifts during a satellite pass, considering a relatively low sampling frequency at the receiver side. First, we perform a model-based pre-compensation of the Doppler shift. Then, based on [11], we estimate the satellite orbital parameters that yield the Doppler shifts closest to the true ones of the entire satellite pass. Finally, we refine the estimated parameters by the well-known simplex method [12].

The paper is organized as follows: in Sec. II we describe the physical model of the observed Doppler shifts based on [7], [8]. In Sec. III we present the utilized signal model for parameter estimation and the challenges involving reducing the sampling frequency and in Sec. IV we discuss the pre-compensation of the received signals based on the physical model for the Doppler shift. In Sec. V we show the results from our proposed method and compare them to when no pre-compensation is applied. Finally, in Sec. VI, we draw the main conclusions from this study.

II. Physical model for Doppler shifts

We describe the utilized physical model to characterize the Doppler shift from a LEO satellite seen by a ground station

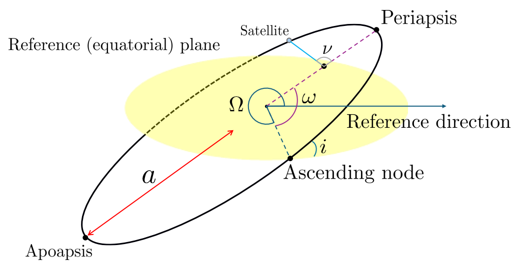

Fig. 1. Graphical overview of orbital parameters.

on Earth, based on [7], [8], for any orbit geometry. Using Kepler's equations, the orbit of a satellite can be characterized by 6 parameters, as illustrated in Fig. 1:

- eccentricity (e): shape of the ellipse, describing how much it is elongated compared to a circle;
- semi-major axis (a): half of the ellipse's major axis;
- inclination (i): angle between the orbital and reference (equatorial) planes;
- longitude of the ascending node (Ω): angle measured from the reference direction to the ascending node (point where the orbit crosses the reference plane);
- argument of periapsis (ω): angle between the ascending node and the periapsis (point where the satellite is closest to the Earth);
- true anomaly (ν): angle between the direction of periapsis and the satellite position, centered on the focus of the ellipse.

In order to calculate the Doppler shift from the satellite to the ground station, it is of interest to describe their velocities in the same coordinate system. We utilize the Earth-centered, Earth-fixed (ECEF) frame, which considers both objects fixed with relation to Earth's rotation. To have such representation, we first provide an orbit description using the Earth-centered inertial (ECI) coordinate system, which does not rotate with the Earth.

In the following, we provide a formulation of the Doppler shift for any orbit shape. However, as circular and near-circular orbits are dominant in LEO constellations, we consider $e = 0$ [6]. Consequently, any point could be declared as the periapsis. Therefore, one can set $\omega = 0$ without lack of generality [13].

A. ECI framework

Since the mass of the Earth M_e is much larger than that of the orbiting satellite, the satellite mean angular velocity is calculated by $n \approx \sqrt{GM_e/a^3}$, where G represents the gravitational constant. This is used to compute the mean anomaly $M = M_0 + n(t - t_0)$, where M_0 is the value of the mean anomaly at time $t = t_0$ [14]. Without loss of generality, we consider $t_0 = 0$.

From M, we determine the eccentric anomaly E by the relation $M = E - e \sin E$. This equation does not have a closed-form solution, but we approximate it by a truncation as in [7, Eq. (17)], where $E = M + e \sin M + \frac{1}{2}e^2 \sin(2M) + \frac{1}{8}e^3 (3 \sin(3M) - \sin M)$. Then, we calculate ν with $\tan\left(\frac{\nu}{2}\right) = \sqrt{\frac{1+e}{1-e}} \tan\left(\frac{E}{2}\right)$. Based on the aforementioned expressions, the distance from the satellite to the center of the Earth is given by $r = \frac{a(1-e^2)}{1+e\cos\nu}$.

From the described variables, we can calculate the satellite position in $[x\ y\ z]^T$ coordinates in the ECI framework at any time instant with

$$\mathbf{r}_{2,\text{ECI}} = r \begin{bmatrix} \cos(\omega+\nu)\cos\Omega - \sin(\omega+\nu)\sin\Omega\cos i \\ \cos(\omega+\nu)\sin\Omega + \sin(\omega+\nu)\cos\Omega\cos i \\ \sin(\omega+\nu)\sin i \end{bmatrix}. \tag{1}$$

Taking the derivative of Eq. (1) with relation to time, the respective velocity is

$$\mathbf{v}_{2,\text{ECI}} = \frac{na}{r} \begin{bmatrix} bl_2\cos E - al_1 \sin E \\ bm_2 \cos E - am_1 \sin E \\ bn_2 \cos E - an_1 \sin E \end{bmatrix}, \tag{2}$$

where

$$\begin{aligned} b &= a\sqrt{1-e^2}, \\ l_1 &= \cos\Omega\cos\omega - \sin\Omega\sin\omega\cos i, \\ m_1 &= \sin\Omega\cos\omega + \cos\Omega\sin\omega\cos i, \\ n_1 &= \sin\omega\sin i, \\ l_2 &= -\cos\Omega\sin\omega - \sin\Omega\cos\omega\cos i, \\ m_2 &= -\sin\Omega\sin\omega + \cos\Omega\cos\omega\cos i, \\ n_2 &= \cos\omega\sin i. \end{aligned}$$

B. ECEF framework

Having the orbit description in the ECI framework, we start the ECEF representation (in $[\hat{x}\ \hat{y}\ \hat{z}]^T$ coordinates) with the position of the ground station

$$\mathbf{r}_{1,\text{ECF}} = r_E \begin{bmatrix} \cos\lambda\cos\phi \\ \sin\lambda\cos\phi \\ \sin\phi \end{bmatrix}, \tag{3}$$

where r_E denotes the radius of the Earth, λ the longitude of the ground station and ϕ its latitude.

To transform the satellite position from ECI to ECEF coordinates, we calculate $\mathbf{r}_{2,\text{ECF}} = \mathbf{T}\mathbf{r}_{2,\text{ECI}}$, where

$$\mathbf{T} = \begin{bmatrix} \cos\theta & \sin\theta & 0 \\ -\sin\theta & \cos\theta & 0 \\ 0 & 0 & 1 \end{bmatrix}. \tag{4}$$

In Eq. (4), $\theta = \theta_0 + \omega_e t$, where θ_0 represents the Greenwich sidereal time at 0h UT and ω_e the Earth's angular speed. Differentiating $\mathbf{r}_{2,\text{ECF}}$ with respect to time, we calculate the satellite velocity in ECEF coordinates. Using the chain rule, we have $\mathbf{v}_{2,\text{ECF}} = \mathbf{T}\mathbf{v}_{2,\text{ECI}} + \dot{\mathbf{T}}\mathbf{r}_{2,\text{ECI}}$, with

$$\dot{\mathbf{T}} = \begin{bmatrix} -\omega_e\sin\theta & \omega_e\cos\theta & 0 \\ -\omega_e\cos\theta & -\omega_e\sin\theta & 0 \\ 0 & 0 & 0 \end{bmatrix}. \tag{5}$$

Defining $\hat{\mathbf{r}}_{3,\text{ECF}} = \frac{\mathbf{r}_{1,\text{ECF}} - \mathbf{r}_{2,\text{ECF}}}{|\mathbf{r}_{1,\text{ECF}} - \mathbf{r}_{2,\text{ECF}}|}$, the relative velocity between the ground station and the satellite is calculated by

$v_r = \mathbf{v}_{2,\text{ECF}} \cdot \hat{\mathbf{r}}_{3,\text{ECF}}$. Finally, the Doppler shift (in Hz) is given by $f_d = \frac{f_c v_r}{c}$, where f_c denotes the carrier frequency and c the speed of light. In our study, a satellite is said to be visible as long as the absolute value of the angle between $-\hat{\mathbf{r}}_{3,\text{ECF}}$ and $\mathbf{r}_{1,\text{ECF}}$ is at most $\pi/2$. The time frame over which a satellite is visible to a ground station is the so-called "visibility window".

III. Signal model

We assume line of sight conditions for the transmission of a pilot signal between a LEO satellite and a ground terminal. Considering P transmitted pilot signals during the visibility window, p-th Doppler-shifted received signal is modeled as

$$y_p[n] = e^{j\varepsilon} e^{j\Omega_{d,p}\left(n-\left(\frac{L-1}{2}\right)\right)} x[n] + w[n], \tag{6}$$

where ε represents a constant phase term, $\Omega_{d,p}$ the normalized Doppler shift frequency, $x[n]$ an all-ones pilot signal vectors of length L, $n = 0, \ldots, L-1$ and $w[n] \sim \mathcal{CN}(0, \sigma_w^2)$. We emphasize that, in this model, the sampling frequency is high enough so that $\Omega_{d,p}$ is approximately constant over the entire received signal.

Relying on linearized versions of $\text{Im}\{y_p[n]\}$, the parameters ε and $\Omega_{d,p}$ can be estimated using a series of linear estimators with increasingly longer data blocks, as proposed in [11]. One of the hyperparameters of this algorithm is Ω_W, denoting the worst-case normalized Doppler shift that can be expected to happen.

For the aforementioned algorithm, the linearization of $\text{Im}\{y_p[n]\} = \sin\left[\varepsilon + \Omega_{d,p}\left(n - \left(\frac{L-1}{2}\right)\right)\right] + \text{Im}\{w[n]\}$ using a first-order Taylor series provides a reasonable approximation for a large amount of samples if $\Omega_{d,p}$ attains a low value. However, for decreasing sampling frequencies at the receiver, $\Omega_{d,p}$ becomes higher and the linearization is not valid for many samples. As a consequence, the variance of the intermediate linear estimators grows significantly (especially in highly noisy scenarios) and the overall estimation procedure may not reach a desirable performance. Nevertheless, if we diligently compensate $y_p[n]$ with some normalized frequency $\Omega_{c,p}$, the compensation error $(\Omega_{d,p} - \Omega_{c,p})$ may be small enough so that one can estimate it using this algorithm and finally find a good estimate for $\Omega_{d,p}$.

IV. Pre-compensation and refinement

As described in Sec. II, the Doppler shift for LEO satellites in circular orbits can be fully characterized by four orbital parameters, namely a, i, Ω and M_0. Estimating them precisely in single input-single output systems, without any prior knowledge of the satellite position, may be a difficult task. The physical model is ambiguous in that different sets of orbital parameters can produce the same Doppler shifts for a given visibility window. We are not concerned with estimating the position of the satellite and, in this section, we take advantage of that to estimate the Doppler shifts even with incorrect estimates of the orbital parameters.

A. *Orbital parameter estimation under model ambiguity*

We first perform a grid search over the parameters a, i, Ω and M_0. For LEO satellites, we consider their ranges to be $a \in [r_E + 200\text{km},\ r_E + 2000\text{km}]$, $i \in [0, 180°]$, $\Omega \in [0, 360°]$, $M_0 \in [0, 360°]$ and compute their Doppler shifts for the analyzed time frame. We discard the orbital parameters that yield non-visible orbits within the given visibility window.

Having all candidate orbital parameters for the considered visibility window, we compensate all $y_p[n]$ signals using the normalized Doppler shifts $\Omega_{c,p}$ yielded by these parameters. The compensated received signals are written as

$$\begin{aligned} y_{c,p}[n] &= e^{-j\Omega_{c,p}\left(n-\left(\frac{L-1}{2}\right)\right)} y_p[n] \\ &= e^{j\varepsilon} e^{j(\Omega_{d,p}-\Omega_{c,p})\left(n-\left(\frac{L-1}{2}\right)\right)} x[n] + w'[n]. \end{aligned} \tag{7}$$

With the algorithm mentioned in Sec. III, we can estimate ε and the compensation error $(\Omega_{d,p} - \Omega_{c,p})$, provided that the latter has a sufficiently low value, and correct the compensation error, finally estimating $\Omega_{d,p}$. Furthermore, the value of Ω_W should be chosen to reflect the worst possible compensation error. We denote the collection of all estimates of ε and $(\Omega_{d,p} - \Omega_{c,p})$ by $\hat{\boldsymbol{\epsilon}}$ and $\hat{\boldsymbol{\Omega}}_e$, respectively.

If the compensation error for all visible received signals is low enough and Ω_W provides a reasonable worst case for it, we can estimate ε consistently. Consequently, var($\hat{\boldsymbol{\epsilon}}$) should be relatively low. Otherwise, the signal model as in Eq. (7) is not applicable and the estimation procedure provides many erroneous estimates, so that var($\hat{\boldsymbol{\epsilon}}$) is high. Thus, we consider good orbital parameters those that give var($\hat{\boldsymbol{\epsilon}}$) below some threshold value, which may depend on the noise level.

Considering all good orbital parameters, the best ones are those that provide the lowest mean(abs($\hat{\boldsymbol{\Omega}}_e$)). As var($\hat{\boldsymbol{\epsilon}}$) is relatively low, the aforementioned signal model is applicable throughout the entire visibility window and we can rely on the estimates for the compensation error. Thus, the orbital parameters that give the lowest mean(abs($\hat{\boldsymbol{\Omega}}_e$)) yield an overall Doppler shift curve that is, on average, close to the true one.

We restate that, starting from the grid search, the best found orbital parameters may not be close to the true ones due to the ambiguity of the physical model. However, the estimated orbital parameters might yield a Doppler shift curve for the whole visibility window that is similar to the true one. We further refine the estimated orbital parameters as follows.

B. *Orbital parameter refinement*

After finding the best orbital parameters from an initial grid search, we further refine them based on the received signals. For this, we apply a derivative-free optimization method, such as the simplex method [12], for which the objective function to be minimized is mean(abs($\hat{\boldsymbol{\Omega}}_e$)). The starting point for this algorithm is the set containing the best orbital parameters and throughout the optimization we run the estimation routine discussed in Sec. III, using all $y_p[n]$ signals.

TABLE I
SYSTEM SIMULATION PARAMETERS

Variable	Value	Variable	Value	Variable	Value	Variable	Value
a	7185km	i	$98.7503°$	Ω	$97.7391°$	M_0	$70.7613°$
λ	$-35.255127°$	ϕ	$-5.812757°$	θ_0	$274.2853°$	T_s	5s
f_c	4GHz	L	300	$f_{s,\text{high}}$	18.42MHz	$f_{s,\text{low}}$	920.91kHz
$\Omega_{d,0}(f_{s,\text{high}})$	0.03	$\Omega_{d,0}(f_{s,\text{low}})$	0.6	$\Omega_{W,\text{high}}$	0.0355	$\Omega_{W,\text{low}}$	0.2

V. Simulation results

We demonstrate our proposed algorithm by means of numerical simulations, where we display the true and estimated Doppler shift curves, with and without the model-based pre-compensation. We show the performance for a relatively high versus a relatively low sampling frequency, denoted as $f_{s,\text{high}}$ and $f_{s,\text{low}}$ respectively. Then, we evaluate the proposed technique in terms of bias and mean square error (MSE) for the strongest (positive) Doppler shift observed during the satellite pass in different signal-to-noise ratio (SNR) regimes and compare to the case where no pre-compensation is applied. The Cramér-Rao lower bound (CRLB), derived in [11], is also assessed for analysis of the MSE. For all simulations, we used $\varepsilon = 1.2$ and 15 points for the grid searches in each dimension. We consider the strongest normalized Doppler shift (as a function of the sampling frequency) $\Omega_{d,0}(f_s)$ to happen when the satellite becomes just visible to the base station [6]. The respective hyperparameters for the normalized Doppler shift estimation are denoted as $\Omega_{W,\text{low}}$ and $\Omega_{W,\text{high}}$. Finally, the satellite transmits a pilot signal every T_s seconds. The simulation parameters are summarized in Tab. I (parameters based on [8]).

A. Simulated Doppler shifts

The simulated numerical results for the given system parameters are shown in Fig. 2, using $f_{s,\text{high}}$ and $\text{SNR} = 15\text{dB}$. In this case, the linearization mentioned in Sec. III provides a good approximation of the sine function for all received signals. It can be seen that the techniques with and without pre-compensation yield practically unbiased estimates for all Doppler shifts within the visibility window. We examine the same situation when using $f_{s,\text{low}}$ in Fig. 3.

As expected, we observe that the estimation without pre-compensation fails at frequencies that yield relatively high normalized Doppler shifts, as the previously discussed linearization does not provide good approximations at such high values of $\Omega_{d,p}$. The model-based pre-compensation enables this linearization, since the compensation error is small enough such that the estimation procedure as in [11] can be carried out as usual. As a result, we can give approximately unbiased Doppler shift estimates for the entire visibility window, even at reduced sampling frequencies.

B. Statistical analysis

The performance of the discussed approaches for the estimation of $\Omega_{d,0}$, the strongest normalized Doppler shift observed by the base station, is assessed in terms of bias and MSE for $\text{SNR} = [-10, 15]\text{dB}$, using 500 realizations. The analysis of our proposed method, for both sampling frequencies, is carried out by applying the estimation procedure in [11] after the optimized pre-compensation. If the compensation error is small enough, we can apply the linear estimation method and reach the CRLB for $\Omega_{d,0}$. In this case, after pre-compensation, we execute the linear estimation method with $\Omega_W = 0.0355$.

In Fig. 4, using $f_{s,\text{high}}$, both methods provide very similar values in terms of bias and MSE, reaching the CRLB for all analyzed SNR values. In particular, the value of $\Omega_{d,0}$ is low

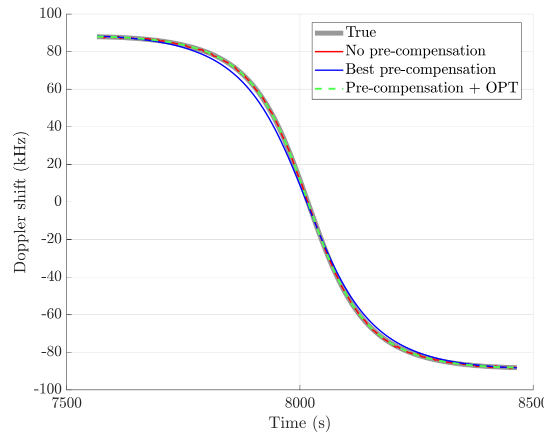

Fig. 2. True and estimated Doppler shifts and best pre-compensation curve for $\text{SNR} = 15\text{dB}$ and $f_{s,\text{high}}$.

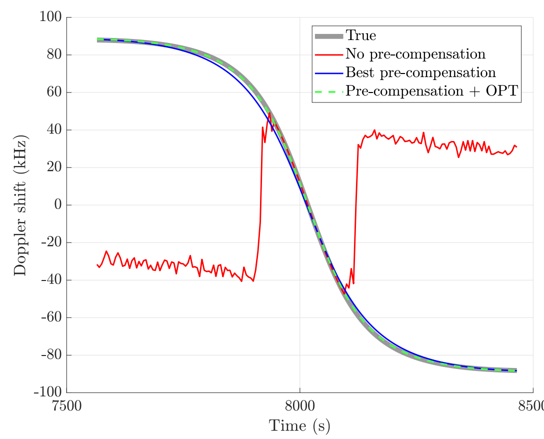

Fig. 3. True and estimated Doppler shifts and best pre-compensation curve for $\text{SNR} = 15\text{dB}$ and $f_{s,\text{low}}$.

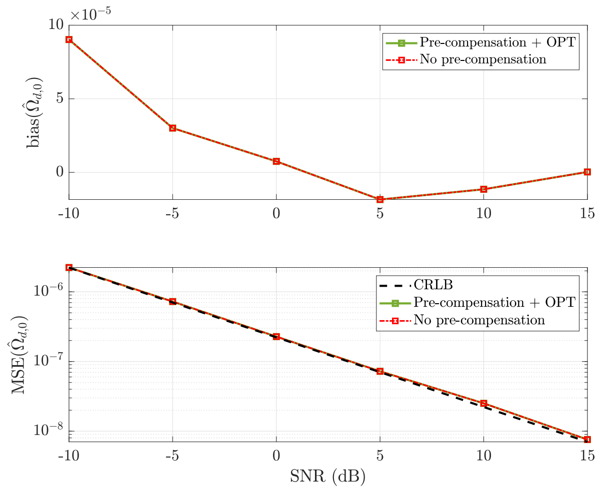

Fig. 4. Bias and MSE of different methods using and $f_{s,\text{high}}$ and varying SNR.

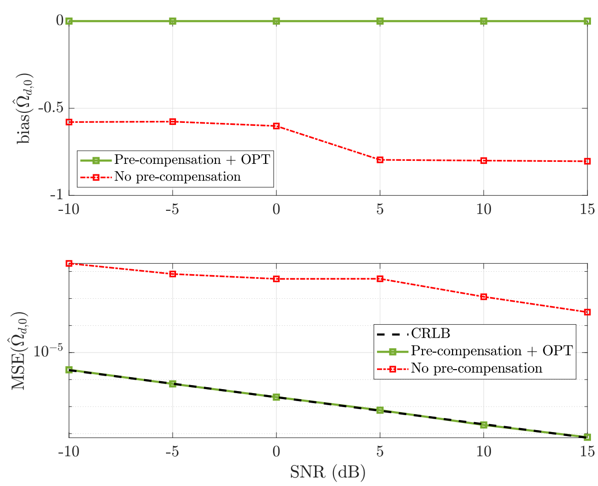

Fig. 5. Bias and MSE of different methods using and $f_{s,\text{low}}$ and varying SNR.

enough such that the linearization provides a good approximation. The pre-compensation yields a small compensation error, which can be estimated with the same variance as when no pre-compensation is applied. Thus, the pre-compensation might not be necessary when using high enough sampling frequencies. The same analysis for $f_{s,\text{low}}$ is given in Fig. 5.

Since the value of $\Omega_{d,0}$ is much higher for $f_{s,\text{low}}$, the linear approximation is no longer valid and the pre-compensation becomes crucial for proper estimation of $\Omega_{d,0}$. Without this first step, the estimates are highly biased and the MSE significantly deviates from the CRLB. With the pre-compensation, however, we can perform the estimations with practically unbiased estimates, reaching the CRLB for a wide range of SNRs.

VI. Conclusions

In this paper, we extend the linear estimation procedure described in [11] to efficiently estimate Doppler shifts in satellite-to-ground communications, while accommodating reduced sampling frequencies. We propose a model-based pre-compensation of the Doppler shift, on the basis of the satellite trajectory and estimating the unknown orbital parameters. Even with ambiguous estimates of the orbital parameters, the pre-compensation can be enough such that the strongest Doppler shifts can be estimated with very low bias and variance reaching the CRLB. Therefore, as a standalone technique, the proposed estimation procedure may be utilized in future satellite communication systems, without the dependence of, e.g., global navigation satellite systems.

Acknowledgment

Funded by the European Union, under ANTERRA 101072363 HORIZON-MSCA-2021-DN-01. Views and opinions expressed are however those of the author(s) only and do not necessarily reflect those of the European Union. Neither the European Union nor the granting authority can be held responsible for them.

References

[1] C. T. Nguyen *et al.*, "Emerging technologies for 6G non-terrestrial-networks: from academia to industrial applications," *IEEE Open Journal of the Communications Society*, vol. 5, pp. 3852–3885, 2024.

[2] F. Rinaldi *et al.*, "Non-terrestrial networks in 5G & beyond: a survey," *IEEE Access*, vol. 8, pp. 165 178–165 200, 2020.

[3] G. Araniti, A. Iera, S. Pizzi, and F. Rinaldi, "Toward 6G non-terrestrial networks," *IEEE Network*, vol. 36, no. 1, pp. 113–120, 2022.

[4] Y. Zhao and S.-G. Haggman, "Sensitivity to Doppler shift and carrier frequency errors in OFDM systems - the consequences and solutions," in *Proceedings of Vehicular Technology Conference - VTC*, vol. 3, 1996, pp. 1564–1568 vol.3.

[5] I. Ali, N. Al-Dhahir, and J. Hershey, "Doppler characterization for LEO satellites," *IEEE Transactions on Communications*, vol. 46, no. 3, pp. 309–313, 1998.

[6] A. Al-Hourani and B. Al Homssi, "Doppler shift distribution in satellite constellations," *IEEE Communications Letters*, vol. 28, no. 9, pp. 2131–2135, 2024.

[7] S. Amiri and M. Mehdipour, "Accurate Doppler frequency shift estimation for any satellite orbit," in *3rd International Conference on Recent Advances in Space Technologies*, 2007, pp. 602–607.

[8] H. Rouzegar and M. Ghanbarisabagh, "Estimation of Doppler curve for LEO satellites," *Wireless Personal Communications*, vol. 108, 10 2019.

[9] D. Tian, Y. Zhao, J. Tong, G. Cui, and W. Wang, "Frequency offset estimation for 5G based LEO satellite communication systems," in *IEEE/CIC International Conference on Communications in China (ICCC)*, 2019, pp. 647–652.

[10] S. Kay, "A fast and accurate single frequency estimator," *IEEE Transactions on Acoustics, Speech, and Signal Processing*, vol. 37, no. 12, pp. 1987–1990, 1989.

[11] A. B. de F. Diniz, T. Eriksson, and U. Gustavsson, "Doppler shift estimation for satellite communications using linear estimators," in *IEEE 25th International Workshop on Signal Processing Advances in Wireless Communications (SPAWC)*, 2024, pp. 686–690.

[12] J. C. Lagarias, J. A. Reeds, M. H. Wright, and P. E. Wright, "Convergence properties of the Nelder–Mead simplex method in low dimensions," *SIAM Journal on Optimization*, vol. 9, no. 1, pp. 112–147, 1998.

[13] I. S. Mohamad Hashim and A. Al-Hourani, "Satellite visibility window estimation using Doppler measurement for IoT applications," *IEEE Communications Letters*, vol. 27, no. 3, pp. 956–960, 2023.

[14] S. A. Klioner, "Basic celestial mechanics," 2016. [Online]. Available: https://arxiv.org/abs/1609.00915